

# Particle-Antiparticle Asymmetries of $\Lambda$ Production in Hadron-Nucleon Collisions

Bo-Qiang Ma

*Department of Physics, Peking University, Beijing 100871, China*

Ivan Schmidt

*Departamento de Física, Universidad Técnica Federico  
Santa María, Casilla 110-V, Valparaíso, Chile*

Jian-Jun Yang

*Departamento de Física, Universidad Técnica Federico  
Santa María, Casilla 110-V, Valparaíso, Chile  
Institut für Theoretische Physik, Universität Regensburg,  
D-93040 Regensburg, Germany and*

*Department of Physics, Nanjing Normal University, Nanjing 210097, China*

## Abstract

The particle-antiparticle asymmetries of  $\Lambda$  production in 250 GeV/c  $\pi^\pm$ ,  $K^\pm$ , and  $p$ -nucleon collisions are studied with two model parametrizations of quark to  $\Lambda$  fragmentation functions. It is shown that the available data can be qualitatively explained by the calculated results in both the quark-diquark model and a pQCD based analysis of fragmentation functions. The differences in the two model predictions are significant for  $K^\pm$  beams, and high precision measurements of the asymmetries with detailed  $x_F$  and  $P_T$  information can discriminate between different predictions.

PACS numbers: 13.85.-t; 13.85.Ni; 13.87.Fh; 14.20.Jn

Much of the recent interest in the structure of the  $\Lambda$  hyperon stems from the fact that its quark structure is rather simple in the naive constituent quark model, since it contains three different quark flavors ( $u, d, s$ ), and furthermore its spin is carried only by the strange quark. Therefore any departure from this picture signals the presence of relativistic and non-perturbative effects. Experimentally the most effective means to investigate the  $\Lambda$  structure is through the quark to  $\Lambda$  fragmentation in various processes [1, 2, 3, 4, 5, 6, 7, 8, 9]. Unfortunately there are still no available measurements about the relations between different flavor-dependent quark to  $\Lambda$  fragmentation functions, such as the relation between the favored and unfavored fragmentation functions, and the relation between the flavor structure of the favored fragmentation functions  $D_u^\Lambda(z)$  and  $D_s^\Lambda(z)$ . Nevertheless there has been recent new measurement of the  $\Lambda$ - $\bar{\Lambda}$  production asymmetries in hadron-nucleon collisions with several different hadron beams at 250 GeV/c by the Fermilab E769 Collaboration [9]. The purpose of this work is to show that the E769 data of  $\Lambda$ - $\bar{\Lambda}$  asymmetries in hadron-nucleon collisions with different hadron beams may provide useful information about the flavor structure of quark to  $\Lambda$  fragmentation functions.

We first look at the formalism for inclusive production of a hadron  $C$  from hadron  $A$  and hadron  $B$  collision process

$$A + B \rightarrow C + X, \quad (1)$$

where the Mandelstam variables  $s$ ,  $t$ , and  $u$  are written as

$$s = (P_A + P_B)^2 = M_A^2 + M_B^2 + 2P_A \cdot P_B, \quad (2)$$

$$t = (P_A - P_C)^2 = M_A^2 + M_C^2 - 2P_A \cdot P_C, \quad (3)$$

$$u = (P_B - P_C)^2 = M_B^2 + M_C^2 - 2P_B \cdot P_C. \quad (4)$$

The experimental cross sections are usually expressed in terms of the experimental variables  $x_F = 2P_L/\sqrt{s}$  and  $P_T$  at a given  $s$ , where  $P_L = x_F\sqrt{s}/2$  and  $P_T$  are the longitudinal and transversal momentum of the produced hadron  $C$  with energy  $E_C = \sqrt{M_C^2 + P_C^2} = \sqrt{M_C^2 + P_L^2 + P_T^2} = \sqrt{M_C^2 + P_T^2 + x_F^2 s/4}$  in the center of mass frame of the collision process, and  $s$  is the squared center of mass energy. In the collinear factorization theorem, the

kinematics of the subprocess  $a + b \rightarrow c + d$  is defined as

$$p_a = x_a P_A, \quad (5)$$

$$p_b = x_b P_B, \quad (6)$$

$$p_c = P_C/z, \quad (7)$$

from which we get the parton level Mandelstam variables  $\hat{s}$ ,  $\hat{t}$ , and  $\hat{u}$

$$\hat{s} = (p_a + p_b)^2 = 2p_a \cdot p_b = x_a x_b s, \quad (8)$$

$$\hat{t} = (p_a - p_c)^2 = -2p_a \cdot p_c = \frac{x_a t}{z}, \quad (9)$$

$$\hat{u} = (p_b - p_c)^2 = -2p_b \cdot p_c = \frac{x_b u}{z}. \quad (10)$$

The cross section can be written in terms of the parton level subprocess as

$$d\sigma = \frac{E_C d^3\sigma^{AB \rightarrow CX}}{d^3\mathbf{P}_C} = \sum_{a,b,c,d} \int \frac{dx_a dx_b dz}{\pi z^2} f_a^A(x_a) f_b^B(x_b) \hat{s} \delta(\hat{s} + \hat{t} + \hat{u}) \frac{d\hat{\sigma}^{ab \rightarrow cd}}{d\hat{t}}(x_a, x_b, z) D_c^C(z), \quad (11)$$

where  $f_a^A(x_a)$  and  $f_b^B(x_b)$  are the parton distributions in the beam hadron  $A$  and target proton  $B$  with Bjorken variables  $x_a$  and  $x_b$  respectively,  $D_c^C(z)$  is the fragmentation function of parton  $c$  into the produced hadron  $C$  with energy fraction  $z$  of hadron  $C$  relative to the scattered quark  $c$ , and  $\frac{d\hat{\sigma}^{ab \rightarrow cd}}{d\hat{t}}(x_a, x_b, z)$  is the subprocess cross section. From the  $\delta(\hat{s} + \hat{t} + \hat{u})$  function, we get the energy fraction  $z$

$$z = -\frac{x_a t + x_b u}{x_a x_b s}, \quad (12)$$

and the two Bjorken variables for quarks  $a$  and  $b$  in hadrons  $A$  and  $B$

$$x_a = \frac{-x_b u}{x_b z s + t}, \quad x_b = \frac{-x_a t}{x_a z s + u}. \quad (13)$$

The integration over  $x_a$  and  $x_b$  can be done for both of  $x_a$  and  $x_b$  in the range  $[0, 1]$ , under the constraint condition  $0 \leq z \leq 1$ , or equivalently, for  $x_a$  and  $x_b$  in the ranges  $[x_a^{min}, 1]$  and  $[x_b^{min}, 1]$  respectively, with

$$x_a^{min} = -\frac{x_b u}{x_b s + t}, \quad x_b^{min} = -\frac{t}{s + u}. \quad (14)$$

The hard scattering framework of Eq. (11) is perturbative QCD based and therefore strictly valid only for high  $P_T \geq 1$  GeV. Nevertheless, it has been recently argued that QCD

factorization is also applicable for semi-inclusive processes at low transverse momentum [10], therefore we make extrapolations to smaller  $P_T$  in this paper for the purpose of illustration. The kinematical expressions that we use, however, are different from the conventional expressions in terms of rapidity [11] and are valid even for small  $P_T$ .

The cross sections of the subprocess at the parton level,  $\hat{\sigma}(\hat{s}, \hat{t}, \hat{u})$ , can be found in Refs. [12]. We adopt the Glück, Reya, and Vogt (GRV) leading order unpolarized parametrization for the nucleon parton distributions [13]. For the parton distributions of the  $K^+$  and  $\pi^-$ , we employ the parametrization forms of Refs. [14] and [15], respectively. The above quantities are well constrained by a vast number of available experimental data, so we can focus our attention on the less known quark to  $\Lambda$  fragmentation functions.

We parametrize the quark to  $\Lambda$  fragmentation functions  $D_q^\Lambda(z)$  by adopting the Gribov-Lipatov relation [16]

$$D_q^\Lambda(z) \propto q^\Lambda(x), \quad (15)$$

in order to connect the fragmentation functions with the quark distribution functions  $q^\Lambda(x)$  of the  $\Lambda$ . More explicitly, we adopt a general form to relate fragmentation and distribution functions, as follows [17]

$$\begin{aligned} D_V^\Lambda(z) &= C_V(z) z^\alpha q_V^\Lambda(z), \\ D_S^\Lambda(z) &= C_S(z) z^\alpha q_S^\Lambda(z), \end{aligned} \quad (16)$$

where a distinction between the valence ( $V$ ) and the sea ( $S$ ) quarks is explicit. The above formulae are always correct, since  $C_V(z)$  and  $C_S(z)$  are in principle arbitrary functions. We should consider Eq. (16) as a phenomenological parametrization for the fragmentation functions of quarks and antiquarks, as follows

$$\begin{aligned} D_q^\Lambda(z) &= D_V^\Lambda(z) + D_S^\Lambda(z), \\ D_{\bar{q}}^\Lambda(z) &= D_S^\Lambda(z). \end{aligned} \quad (17)$$

Three options were found [17] to fit quite well the available experimental data of proton production in  $e^+e^-$  inelastic annihilation: (1)  $C_V = 1$  and  $C_S = 0$  for  $\alpha = 0$ ; (2)  $C_V = C_S = 1$  for  $\alpha = 0.5$ ; and (3)  $C_V = 1$  and  $C_S = 3$  for  $\alpha = 1$ . We adopt these three options to reflect the relation between unfavored and favored fragmentation functions of the  $\Lambda$ .

There is no direct measurement of the quark distributions of the  $\Lambda$ . But we can relate the quark distributions between the proton and the  $\Lambda$  by assuming SU(3) symmetry between

the proton and the  $\Lambda$  [18]

$$\begin{aligned} u_V^\Lambda(x) &= d_V^\Lambda(x) = \frac{1}{6}u_V(x) + \frac{4}{6}d_V(x), \\ s_V^\Lambda(x) &= \frac{2}{3}u_V(x) - \frac{1}{3}d_V(x), \end{aligned} \tag{18}$$

for valence quarks, and

$$\begin{aligned} \bar{u}^\Lambda(x) &= \bar{d}^\Lambda(x) = \frac{1}{2}[\bar{u}(x) + \bar{s}(x)], \\ \bar{s}^\Lambda(x) &= \bar{d}(x), \end{aligned} \tag{19}$$

for sea quarks. We adopt the GRV parametrization [13] of the quark distributions  $q(x)$  of the nucleon. In this way, we get a complete set of quark distributions in the  $\Lambda$  with both valence and sea quark distributions.

It is well known that the flavor structure of  $u$  and  $d$  quark distributions of the proton is different between the quark-diquark model [19, 20, 21] and a pQCD based analysis [22, 23]: the quark-diquark model predicts that  $d(x)/u(x) \rightarrow 0$  at  $x \rightarrow 1$  whereas a pQCD based approach predicts that  $d(x)/u(x) \rightarrow 1/5$ . A discrimination between the two models requires very high precision measurement of the structure functions at large  $x$  and is difficult. On the other hand, it has been also shown [2] that this flavor structure of the quark distributions at large  $x$  is even more significant in the case of the  $\Lambda$ , with a large difference between the ratio of  $u^\Lambda(x)/s^\Lambda(x)$ : the quark-diquark model predicts that  $u^\Lambda(x)/s^\Lambda(x) \rightarrow 0$  at  $x \rightarrow 1$ , whereas the pQCD based approach predicts that  $u^\Lambda(x)/s^\Lambda(x) \rightarrow 1/2$ . This will produce a large difference in the ratio of fragmentation functions  $D_u^\Lambda(z)/D_s^\Lambda(z)$ , which might be more easily accessible experimentally via quark to  $\Lambda$  fragmentation [24].

The valence quark distributions of the  $\Lambda$  in the quark-diquark model and the pQCD based analysis have been explicitly studied [2, 3, 25] and we adopt the parametrizations given in Ref. [25]. To describe the  $\bar{\Lambda}$  fragmentation, it is important to take into account the sea contributions in the model construction. In order to use the sea quark distributions from other parametrization while still keeping the flavor structure of the valence quarks as predicted in the two models, we re-scale the valence quark distributions by a factor of  $u_{V,SU(3)}^\Lambda(x)/u_{V,th}^\Lambda(x)$ , where the subscript “ $SU(3)$ ” denotes the valence quark distributions of the  $\Lambda$  in the  $SU(3)$  symmetry model [18] and “ $th$ ” denotes the corresponding quantities predicted in the quark-diquark model or the pQCD based analysis [25]. This is done in order to normalize the  $\Lambda$  quark distributions to well known proton quark distribution parametrizations. Notice that the valence  $u$ -quark distribution then becomes that of the  $SU(3)$  model, while the others get a rescaling factor. In this way we can adopt the sea quark distributions

from the SU(3) symmetry model as the sea distributions in the quark-diquark model and the pQCD based analysis, to reflect the contribution from the unfavored fragmentation. Thus we get another two sets of quark to  $\Lambda$  fragmentation functions, denoted as the quark-diquark model and the pQCD based analysis later on. This procedure is done with the main motivation of constructing realistic quark to  $\Lambda$  phenomenological fragmentation functions, which has some features coming from specific theoretical arguments, i.e., the quark-diquark model and the pQCD based analysis.

With all of the above mentioned subprocess cross sections at the parton level, parton distributions for both the beam and the target, and also the quark to  $\Lambda$  fragmentation functions, we can calculate the  $x_F$ -dependent  $\Lambda$ - $\bar{\Lambda}$  asymmetries in hadron-nucleon collisions

$$A(x_F) = \int_{P_T^{min}}^{P_T^{max}} d^2\vec{P}_T \left[ \frac{d^3\sigma^\Lambda}{d^3p_\Lambda} - \frac{d^3\sigma^{\bar{\Lambda}}}{d^3p_{\bar{\Lambda}}} \right] / \int_{P_T^{min}}^{P_T^{max}} d^2\vec{P}_T \left[ \frac{d^3\sigma^\Lambda}{d^3p_\Lambda} + \frac{d^3\sigma^{\bar{\Lambda}}}{d^3p_{\bar{\Lambda}}} \right], \quad (20)$$

and those with  $P_T^2$ -dependence

$$A(P_T^2) = \int_{x_F^{min}}^{x_F^{max}} dx_F \left[ \frac{d^3\sigma^\Lambda}{d^3p_\Lambda} - \frac{d^3\sigma^{\bar{\Lambda}}}{d^3p_{\bar{\Lambda}}} \right] / \int_{x_F^{min}}^{x_F^{max}} dx_F \left[ \frac{d^3\sigma^\Lambda}{d^3p_\Lambda} + \frac{d^3\sigma^{\bar{\Lambda}}}{d^3p_{\bar{\Lambda}}} \right]. \quad (21)$$

We do not introduce any additional parameters to fit the data for the input quantities.

The E769 Collaboration measured the asymmetries with 250 GeV/c  $\pi^\pm$ ,  $K^\pm$ , and  $p$  beams on the proton target. The data are expressed as functions of  $x_F$  and  $P_T^2$  over the ranges  $-0.12 \leq x_F \leq 0.12$  and  $0 \leq P_T^2 \leq 3$  (GeV/c)<sup>2</sup> for positively charged beam, and  $-0.12 \leq x_F \leq 0.4$  and  $0 \leq P_T^2 \leq 10$  (GeV/c)<sup>2</sup> for negatively charged beam. In fact, the  $x_F$ -dependence was measured without  $P_T^2$  cut, and the  $P_T^2$ -dependence was measured without  $x_F$  cut. Notice that in the  $P_T$  integration we have considered the small ( $\leq 1$  GeV) region, where the hard scattering formalism is not strictly valid. We have checked that the final results are not really sensitive to this lower limit.

In the theoretical calculation, we need to set the limits of  $P_T^{min}$  and  $P_T^{max}$  for the  $x_F$ -dependence, and of  $x_F^{min}$  and  $x_F^{max}$  for the  $P_T^2$ -dependence. We will choose the above mentioned ranges in the calculation. In Fig. 1, we plot the calculated results for the  $x_F$ -dependent asymmetries  $A(x_F)$ , and find that both the quark-diquark model and the pQCD based analysis can explain the trend of the data. The quark-diquark model seems to be somewhat more favored by the data for  $K^\pm$  beams, especially at large  $x_F$ . The differences between the quark-diquark model and the pQCD based analysis can be understood by the fact that

$x_F \approx x_a - x_b$  in the Bjorken limit, and that the large  $x_F$  behaviors is mainly controlled by the  $\bar{s}$  and  $s$  quark fragmentation of the beam at large  $x_F$ . In the quark-diquark model, the  $s$  quark fragmentation dominates over the light-flavor quark fragmentation. Therefore the dominant  $\bar{s}$  fragmentation of the  $K^+$  beam favors  $\bar{\Lambda}$  production, whereas the dominant  $s$  fragmentation of the  $K^-$  beam favors  $\Lambda$  production. This can explain why the asymmetries  $A(x_F)$  for the  $K^-$  beam is negative at large  $x_F$  whereas they are positive for the  $K^+$  beam. From the different flavor structure of  $D_u^\Lambda(z)/D_s^\Lambda(z) \rightarrow 0$  in the quark-diquark model and of  $D_u^\Lambda(z)/D_s^\Lambda(z) \rightarrow 1/2$  in the pQCD based analysis, we can explain why the quark-diquark model predicts large magnitude for the asymmetries  $A(x_F)$  at large  $x_F$  for  $K^\pm$  beams, since the  $s$  quark fragmentation dominates over the light-flavor fragmentation in the quark-diquark model. We thus conclude that the large  $x_F$  behavior of the  $\Lambda$ - $\bar{\Lambda}$  asymmetries can discriminate between the two model predictions. We present in Fig. 2 of the calculated results of the  $A(x_F)$  asymmetries with two different options of  $P_T$ -cut: the integrated ranges of  $[(P_T^{\min})^2, (P_T^{\max})^2]$  are  $[0, 5]$  and  $[5, 10]$  respectively. We find that the trend in the  $x_F$ -dependence does not change much for the two options, although the magnitudes are different.

We also plot the calculated results for the  $P_T^2$ -dependent asymmetries  $A(P_T^2)$  in Fig. 3, and find that both the quark-diquark model and the pQCD based analysis can explain the  $P_T^2$ -dependence trend, but the results differ slightly in magnitude from the data. The reason is that the asymmetries  $A(P_T^2)$  are very sensitive to the  $x_F$  integration range  $[x_F^{\min}, x_F^{\max}]$ , and we cannot reproduce exactly the real  $[x_F^{\min}, x_F^{\max}]$  of the data. This is supported by Fig. 4, in which we plot the calculated results of  $A(P_T^2)$  with two options of  $x_F$ -cut: the integrated ranges of  $[x_F^{\min}, x_F^{\max}]$  are  $[-0.12, 0]$  and  $[0, 0.12]$  respectively. We find that the magnitude of the asymmetries  $A(P_T^2)$  differ significantly for the two options, whereas the trend of the  $P_T^2$ -dependence is similar. Thus both the quark-diquark model and the pQCD based analysis can explain the  $P_T^2$ -dependence in trend, but the exact magnitude is sensitive to the  $x_F$ -cut. Therefore we conclude that the magnitude of  $A(P_T^2)$  with detailed  $x_F$ -cut information is important for the purpose of distinguishing between different model predictions. Thus far we only expect our formalism to work for asymmetries, rather than for cross sections. In this last case there are questions of normalization and evolution which are not present for asymmetries.

In summary, we showed in this work that the  $\Lambda$ - $\bar{\Lambda}$  asymmetries in hadron-nucleon colli-

sions can provide information about the flavor structure of quark to  $\Lambda$  fragmentation functions. Both the quark-diquark model and a pQCD based analysis can explain the available data qualitatively. We also showed that the two models give significant different predictions for the magnitude of the  $x_F$ -dependent asymmetries at large  $x_F$  for  $K^\pm$  beams. Thus high precision measurements of the asymmetries with detailed  $x_F$ -cut and  $P_T$ -cut information are important to discriminate between different predictions.

### **Acknowledgments**

We acknowledge the helpful communication with H. da Motta for some detailed information of the E769 data. This work is partially supported by National Natural Science Foundation of China under Grant Numbers 10025523 and 90103007, by Fondecyt (Chile) grant 1030355, by Alexander von Humboldt-Stiftung (J.-J. Yang), and by Foundation for University Key Teacher by the Ministry of Education (China).



- 
- [1] B.-Q. Ma, I. Schmidt, J. Soffer, J.-J. Yang, Phys. Rev. D **64** (2001) 014017, and references therein.
- [2] B.-Q. Ma, I. Schmidt, J.-J. Yang, Phys. Lett. B **477** (2000) 107.
- [3] B.-Q. Ma, I. Schmidt, J.-J. Yang, Phys. Rev. D **61** (2000) 034017.
- [4] ALEPH Collaboration, D. Buskulic, *et al.*, Phys. Lett. B **374** (1996) 319.
- [5] OPAL Collaboration, K. Ackerstaff, *et al.*, Eur. Phys. J. C **2** (1998) 49.
- [6] HERMES Collaboration, A. Airapetian, *et al.*, Phys. Rev. D **64** (2001) 112005.
- [7] E665 Collaboration, M.R. Adams, *et al.*, Eur. Phys. J. C **17** (2000) 263.
- [8] NOMAD Collaboration, P. Astier, *et al.*, Nucl. Phys. B **588** (2000) 3.
- [9] E769 Collaboration, G.A. Alves, *et al.*, Phys. Lett. B **559** (2003) 179.
- [10] X.-D. Ji, J.-P. Ma, F. Yuan, hep-ph/0404183.
- [11] For the conventional formalism of kinematics, see, e.g., J. F. Owens, Rev. Mod. Phys. **59** (1987) 465.
- [12] C. Bourrely, J. Soffer, F.M. Renard, P. Taxil, Phys. Rep. **177** (1989) 319.
- [13] M. Glück, E. Reya, A. Vogt, Z. Phys. C **67** (1995) 433.
- [14] M. Glück, E. Reya, M. Stratmann, Eur. Phys. J. C **2** (1998) 159.
- [15] M. Glück, E. Reya, I. Schienbein, Eur. Phys. J. C **10** (1999) 313.
- [16] V.N. Gribov, L.N. Lipatov, Phys. Lett. B **37** (1971) 78;  
V.N. Gribov, L.N. Lipatov, Sov. J. Nucl. Phys. **15** (1972) 675;  
S.J. Brodsky, B.-Q. Ma, Phys. Lett. B **392** (1997) 452;  
V. Barone, A. Drago, B.-Q. Ma, Phys. Rev. C **62** (2000) 062201(R).
- [17] B.-Q. Ma, I. Schmidt, J. Soffer, J.-J. Yang, Phys. Lett. B **547** (2002) 245.
- [18] B.-Q. Ma, I. Schmidt, J. Soffer, J.-J. Yang, Phys. Rev. D **65** (2002) 034004.
- [19] R.P. Feynman, *Photon Hadron Interactions* (Benjamin, New York, 1972), p. 150.
- [20] F.E. Close, Phys. Lett. **43 B** (1973) 422; Nucl. Phys. B **80** (1974) 269;  
R. Carlitz, Phys. Lett. B **58** (1975) 345;  
J. Kaur, Nucl. Phys. B **128** (1977) 219;  
A. Schäfer, Phys. Lett. B **208** (1988) 175;  
F.E. Close, A.W. Thomas, Phys. Lett. B **212** (1988) 227;

- N. Isgur, Phys. Rev. D **59** (1999) 034013.
- [21] B.-Q. Ma, Phys. Lett. B **375** (1996) 320.
- [22] G.R. Farrar, D.R. Jackson, Phys. Rev. Lett. **35** (1975) 1416.
- [23] S.J. Brodsky, M. Burkardt, I. Schmidt, Nucl. Phys. B **441** (1995) 197.
- [24] J.-J. Yang, Phys. Lett. B **526** (2002) 50.
- [25] B.-Q. Ma, I. Schmidt, J. Soffer, J.-J. Yang, Phys. Rev. D **62** (2000) 114009.

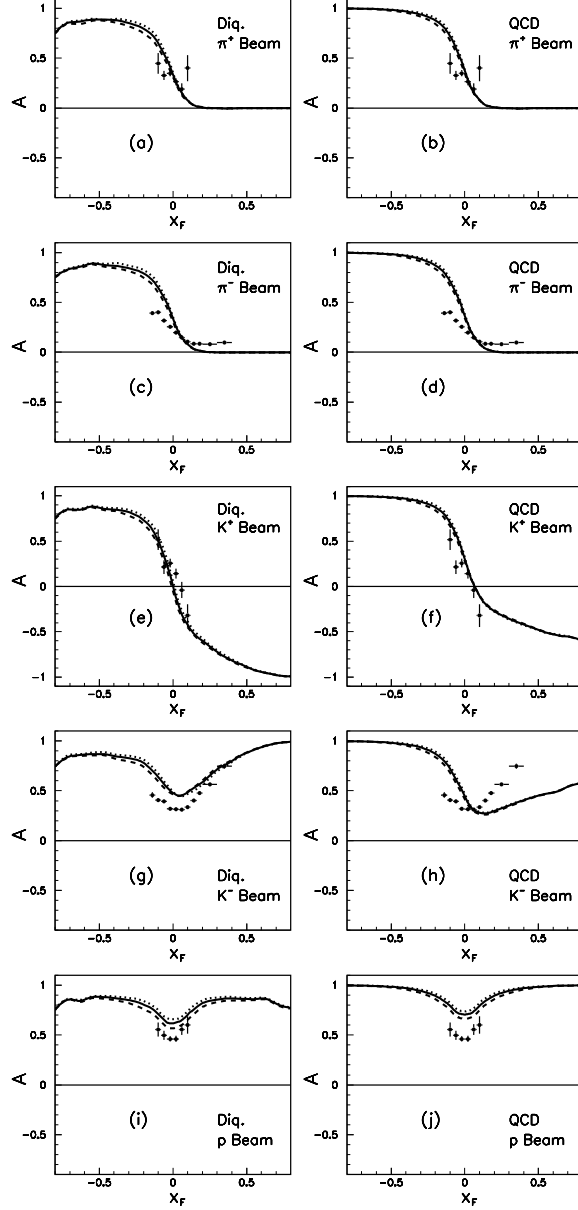


FIG. 1: The prediction for the  $\Lambda$  production asymmetries vs  $x_F$  for various incident beams, and with three options for the contribution from unfavored fragmentation: (1) the dotted curve is for  $C_V = 1$  and  $C_S = 0$ ,  $\alpha = 0$ ; (2) the solid curve is for  $C_V = C_S = 1$ ,  $\alpha = 0.5$ ; and (3) the dashed curve is for  $C_V = 1$  and  $C_S = 3$ ,  $\alpha = 1$ . The left row figures correspond to results from the quark-diquark model, and the right row figures correspond to results from a pQCD based analysis. The integration range of  $P_T^2$  is  $0 \leq P_T^2 \leq 3$   $(\text{GeV}/c)^2$  for positively charged beams, and  $0 \leq P_T^2 \leq 10$   $(\text{GeV}/c)^2$  for negatively charged beams. The experimental data are taken from Ref. [9].

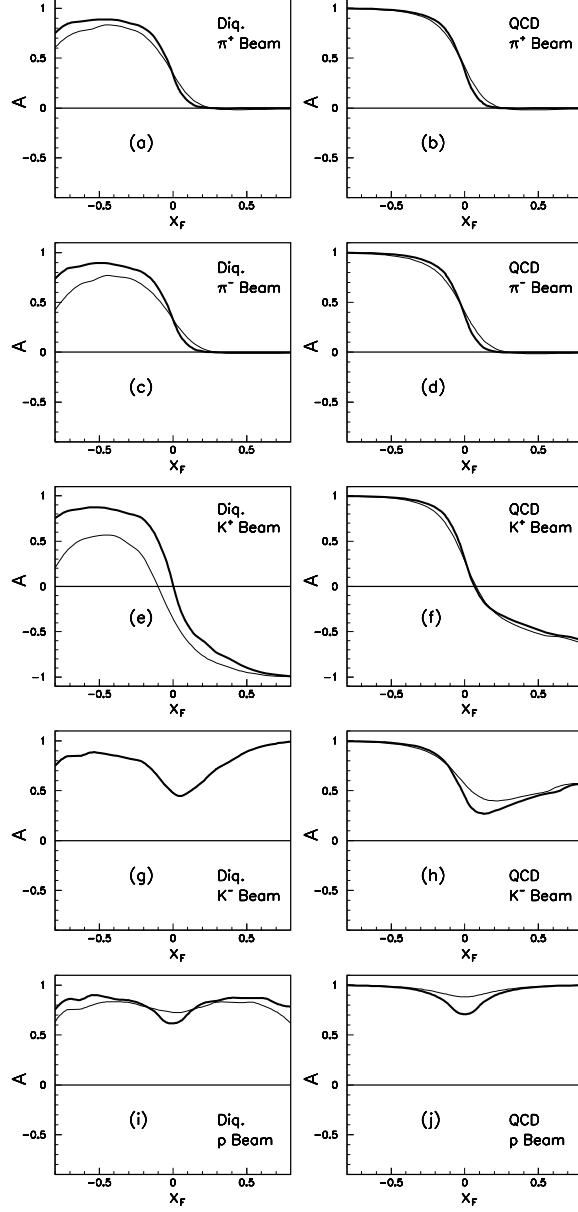


FIG. 2: The same as in Fig. 1, using only the contribution from unfavored fragmentation with  $C_V = C_S = 1$  for  $\alpha = 0.5$ . The integration range of  $p_T^2$  is  $[0, 5]$   $\text{GeV}^2$  for the thick solid curves and  $[5, 10]$   $\text{GeV}^2$  for the thin solid curves.

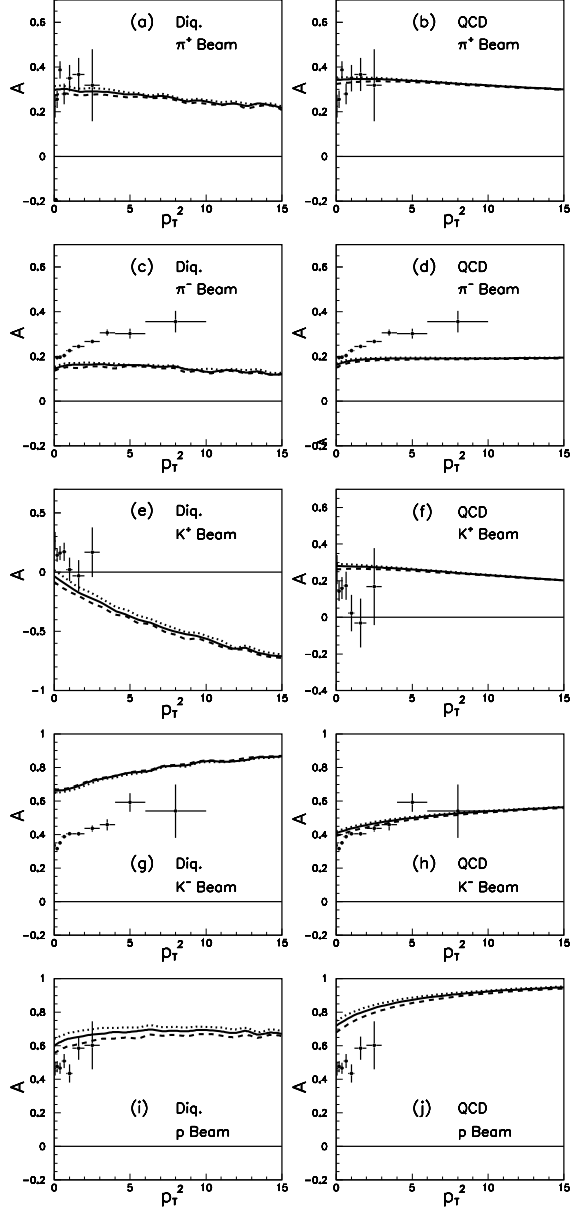


FIG. 3: The prediction of  $\Lambda$  production asymmetries vs  $P_T^2$  for various incident beams with the dotted, solid, and dashed curves corresponding to the three options for the unfavored fragmentation as in Fig. 1. The integration range of  $x_F$  is  $-0.12 \leq x_F \leq 0.12$  for positively charged beams, and  $-0.12 \leq x_F \leq 0.4$  for negatively charged beams. The experimental data are taken from Ref. [9].

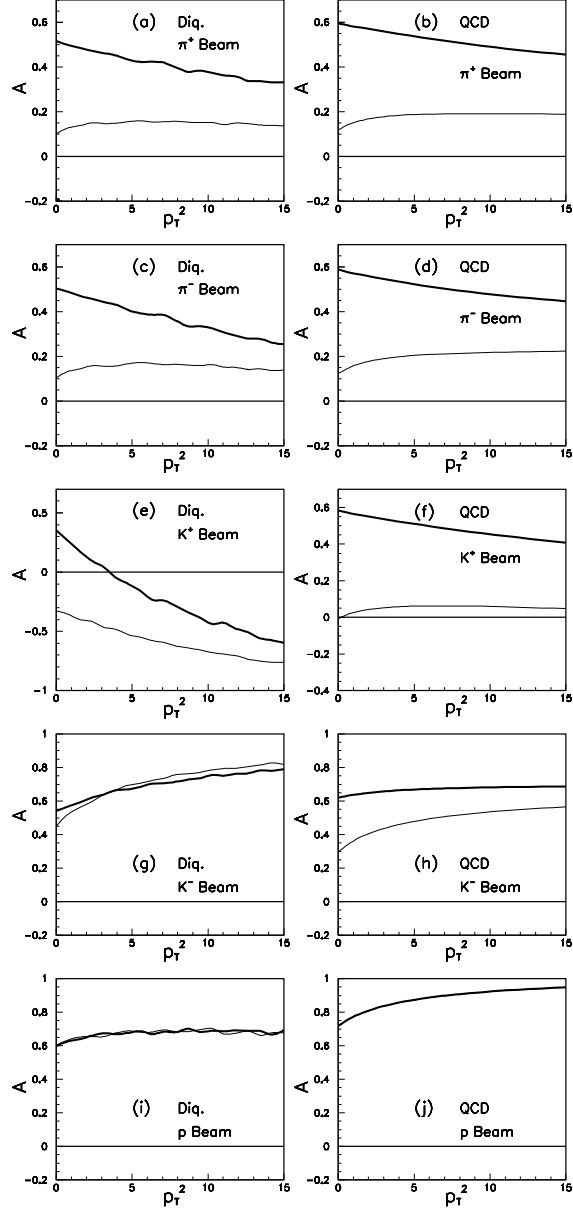


FIG. 4: The same as in Fig. 3 by using only the contribution from unfavored fragmentation with  $C_V = C_S = 1$  for  $\alpha = 0.5$ . The integration range of  $x_F$  is  $[-0.12, 0.0]$  for the thick solid curves and  $[0.0, 0.12]$  for the thin solid curves.